

Vacuum-free fabrication of organic solar cell on assembled glass substrates

Hao-Chun Yang^{a,1}, Wusong Zha^{b,1}, Chia-Ning Weng^{c,1}, Chao-Hsuan Chen^d, Hsiao-Wen Zan^d, Kuan-Wei Su^c, Qun Luo^{b,**}, Chang-Qi Ma^b, Yu-Chiang Chao^{e,*}, Hsin-Fei Meng^a

^a Institute of Physics, National Chiao Tung University, Hsinchu, 300, Taiwan

^b Printable Electronic Research Center, Suzhou Institute of Nano-Tech and Nano-Bionics, Chinese Academy of Sciences (CAS), China

^c Department of Electrophysics, National Chiao Tung University, Hsinchu, 300, Taiwan

^d Department of Photonics, National Chiao Tung University, Hsinchu, Taiwan

^e Department of Physics, National Taiwan Normal University, Taipei, 106, Taiwan

ARTICLE INFO

Keywords:

Organic solar cells
Vacuum-free
Blade-coating
Assembled glass substrates

ABSTRACT

Vacuum-free fabrication is essential to realize large-scale production of organic solar cells. Blade-coating and printing are important solution-processing techniques to realize this idea. Preparation devices on large substrates is important for mass production; however, it is not easy to handle large substrates during fabrication procedures. In this work, we demonstrate a fabrication method for all-solution vacuum-free organic solar cells on an assembled glass substrates. Small pieces of glasses were assembled into a mosaic of larger total size for device fabrication. A gap-pre-filling method was also developed to realize uniform thickness distribution. For the device with blade-coated ZnO electron transport layer, blade-coated active layer, spray-coated hole transport layer and spray-coated top electrode, power conversion efficiency of 4.19% is obtained. This showed that, by combining spray and blade coating, ultimate scale of the vacuum-free fabrication of OPV on glass substrate will not be limited by the substrate size itself, and can be scaled up to multi-meter by assembling the glasses into a mosaic.

1. Introduction

Organic solar cell, or organic photovoltaic (OPV), is considered as a promising new generation of solar cell technology [1,2]. OPV has the advantages of light-weight, semi-transparency, beautiful color, and absence of toxic heavy metals. One of the uniqueness of OPV is the possibility of all-solution vacuum-free fabrication starting from commercial transparent conducting indium-tin-oxide (ITO) substrates [3,4]. The electron transport layer, active-absorbing layer can be deposited by blade coating [5,6] or slot-die coating [7,8]. The hole transport layer can be deposited by spray coating or blade coating [9,10]. Finally the top electrode can be deposited by spray coating of silver nanowires (Ag NW) [11,12]. There are two choices for the ITO substrate: the glass or plastic. The plastic substrate has the advantages of large-area roll-to-roll process, but it has the drawback of weak air barrier and lower lifetime in general. As for the glass substrate, it has a superior air barrier but is difficult to handle in large area because of the rigid and fragile nature of glass. In principle, the vacuum-free fabrication like blade coating or

spray coating can extended easily to scales over 10 m. But a single piece of glass with such dimension will be impractical for production and transportation. It is therefore important to develop a method to combine the large-area fabrication and the practical glass substrate size.

In this work we propose a new method for solution fabrication of OPV on assembled glass substrates instead of a single glass. Small pieces of square glasses can be assembled into a mosaic of larger total size. If the fabrication can be made successfully on such an assembly, the glass substrates can be individually handled conveniently for further steps like transportation and encapsulation. For example, individual glass can be chosen to be of A4 size (20 cm × 30 cm). 40 pieces can be assembled into a 4 × 10 mosaic. The total size will be 80 cm × 300 cm. Blade or spray coating of this size is acceptable, but a single glass of this size is difficult to handle. However in order to realize a solution fabrication on an assembly, one must overcome the problem of inevitable solution leakage into the gaps of the mosaic. Such leakage leads to poor film uniformity.

By pre-filling of the glass by the solution, we demonstrate that good

* Corresponding author.

** Corresponding author.

E-mail addresses: qluo2011@sinano.ac.cn (Q. Luo), ycchao@ntnu.edu.tw (Y.-C. Chao).

¹ Hao-Chun Yang, Wusong Zha, and Chia-Ning Weng contributed equally to this work.

film uniformity can be achieved by blade coating of the active bulk-heterojunction (BHJ) layer of OPV. Small glass substrate of 2.5 cm \times 2.5 cm is used to verify this concept. The hole transport layer and the top electrode is deposited by spray coating. The power conversion efficiency of 4.19% is obtained. This showed that, by combining spray and blade coating, ultimate scale of the vacuum-free fabrication of OPV on glass substrate will not be limited by the substrate size itself, and can be scaled up to multi-meter by assembling the glasses into a mosaic.

2. Results and discussion

To facilitate the production and transportation, a method for large-area fabrication based on small-sized glass substrates was developed

in this work. Small-area glass substrate (2.5 cm \times 2.5 cm) with pre-patterned ITO was used to demonstrate this method, as shown in Fig. 1(a). The ITO electrodes are indicated by the blue regions and the active areas of the 4 devices are determined by the cross-over region of ITO electrode and top electrode (dashed squares). 4 pieces of small-area glass substrates were assembled into a 2 \times 2 mosaic, which was fixed by outer glass substrates as the frame, as shown in Fig. 1(b) and c.

In this work, the preparation of ZnO, photoactive layer PTB7-Th (PBDTTT-EFT):PC₇₀BM, and PEDOT:PSS on assembled glass substrates was done by blade coating. In the blade coating procedures, the solution was dropped at the gap between the blade coater and the substrate by a micropipette. Because of the capillary, the solution will be distributed through all the gap space. While blading coating, the substrates were

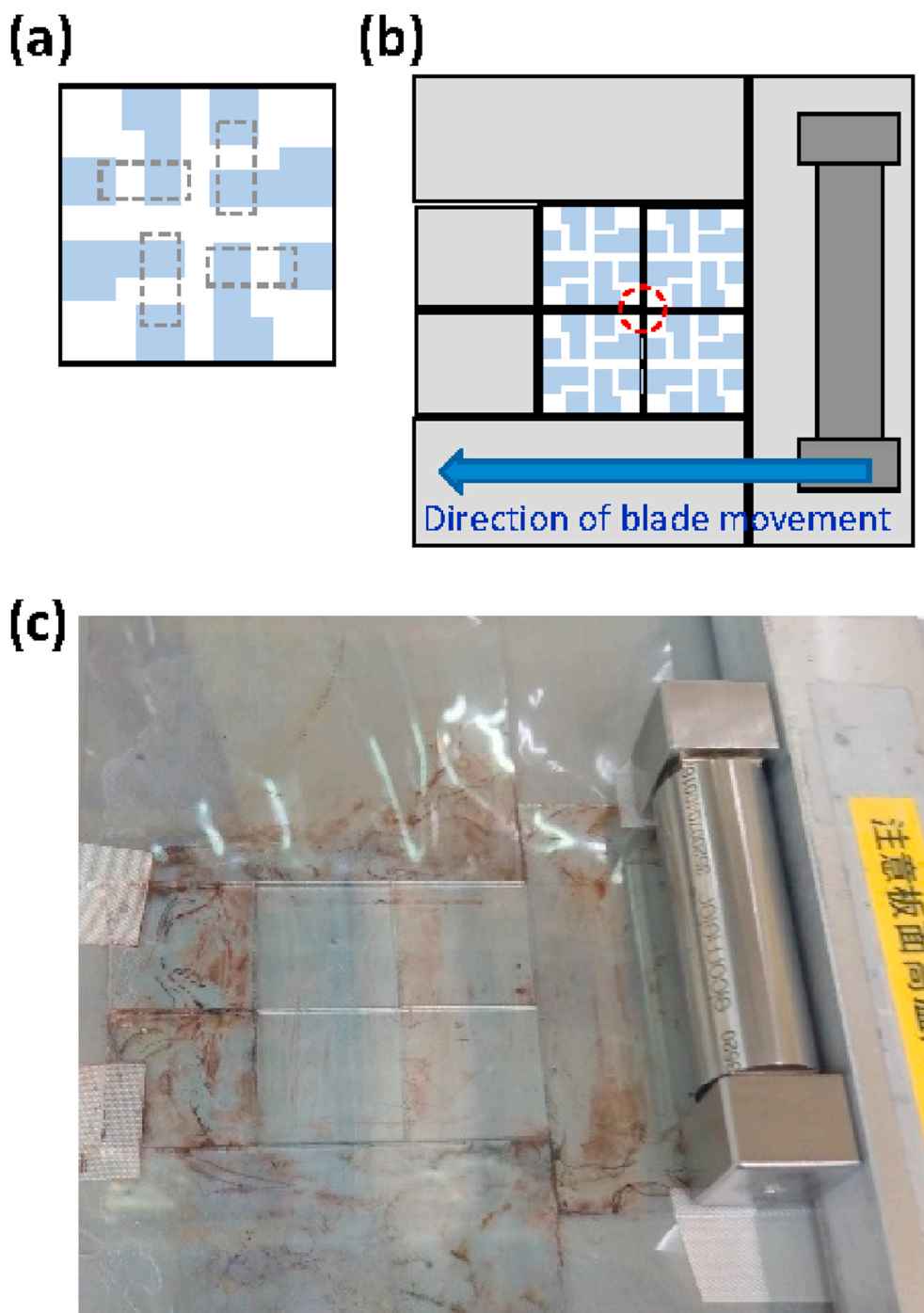


Fig. 1. The schematic diagram of (a) the patterned ITO glass substrate and (b) the blade coating procedure. (c) The photograph of the blade coater.

simultaneously heated from top (hot wind) and bottom (hotplate) to quickly dry the solution. When there is only one substrate, the dosage of the solution and the speed and acceleration of the blade coater were used to control the film thickness [6,10]. However, when there are many substrates, inevitable solution leakage into the gaps between different glasses leads to non-uniform thickness. As shown in Fig. 2(a), the thickness of the photoactive layer taken at different locations on the four glass substrates are indicated. The thickness ranges from about 45 nm to 90 nm, which is too thin to realize high performance devices. The distribution of the material thickness on different substrates was crucial for device performance and mass production. Therefore, the thickness of these materials was investigated as a first step.

To increase the thickness and decrease the thickness variation, a small amount of the solution was put at the center (red dashed circle in Fig. 1) of the 2 × 2 cm mosaic. The solution will spread along the gaps between glass substrates, and the gaps are filled with the solution. We name this process as the gap pre-filling process. With this gap pre-filling process, the blade coating for the photoactive layer leads to a thicker film about 83 nm–110 nm, as shown in Fig. 2(b). Similarly, with the gap pre-filling process, the blade-coated PEDOT:PSS layer also show reasonable thickness, as shown in Fig. 2(c). As for the ZnO layer, the thickness of ZnO is estimated to be less than 10 nm since the measured thickness was in the noise level of the surface profiler. Even with the gap-pre-filling process, the ZnO thickness is too thin to be determined exactly.

After the optimization of coating technology of the organic active layer, we moved forwards to the fabrication of full-coated organic solar cells through combining the blade coated ZnO cathode buffer layer, the organic active layer, and the spray-coated hole extraction layers (HTLs) and anode [13,14]. To optimize the device structure of the full-coated solar cells, different HTLs, vacuum-evaporated MoO₃ (e-MoO₃), solution-processed MoO₃ (s-MoO₃), and PEDOT:PSS were used. The device structure and energy band diagram are shown in Fig. 3. For the top anode, Ag nanowires (Ag NWs) networks were deposited on the top HTLs through spray coating. Since the Ag NWs has high visible transparency as higher than 85%, these devices with Ag NWs electrode are semi-transparent. Fig. 4 shows the J-V characteristics and the EQE spectra of these devices, and corresponding performance parameters are listed in Table 1. The performance of the reference cells, in which the top electrode was prepared by thermal evaporation, are also shown in Fig. 5 for comparison. The device with evaporated MoO₃/Al top electrode shown an efficiency of 7.58%, while the device with only evaporated Al top electrode shown an extremely poor efficiency of 0.87%. Both the open circuit voltage (V_{oc}) and fill factor (FF) of the device with evaporated Al are far away lower than the device with evaporated MoO₃/Al, indicating a HTL with higher work function is required.

As the Ag NWs was printed on the top of e-MoO₃, the V_{oc} increased

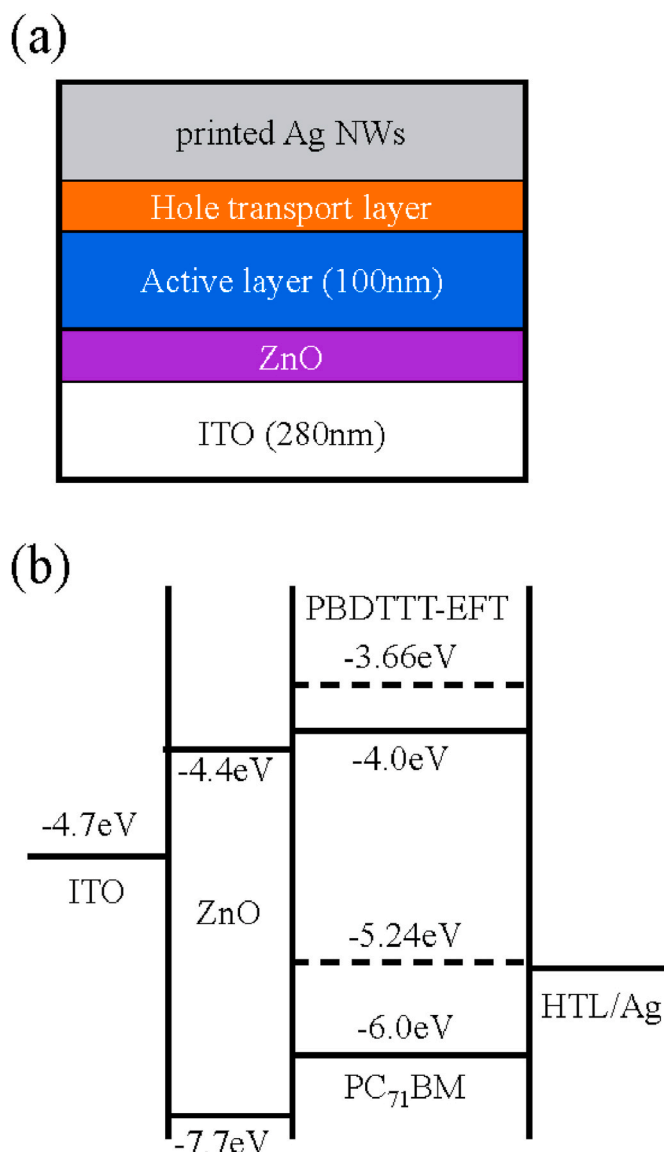


Fig. 3. (a) The device structure and (b) the energy band diagram of the device.

to 0.8 V, which is nearly comparable with the control cell. However, the FF of this cell is lower than 0.4, and as a result a low efficiency of 3.14% is observed. For the device with s-MoO₃ HTLs, the optimized efficiency

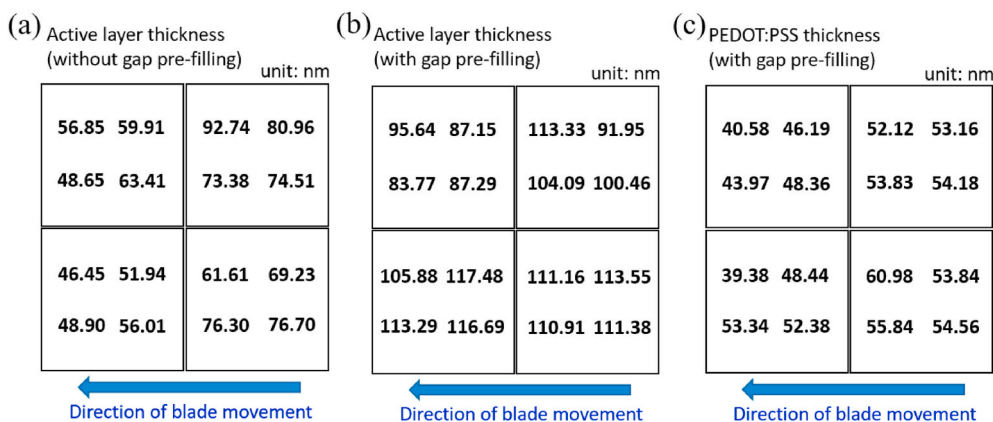


Fig. 2. (a) The distribution of the active layer thickness on different substrates without gap pre-filling process. (b) The distribution of the active layer thickness on different substrates with gap pre-filling process. (c) The distribution of the PEDOT:PSS thickness on different substrates with gap pre-filling process.

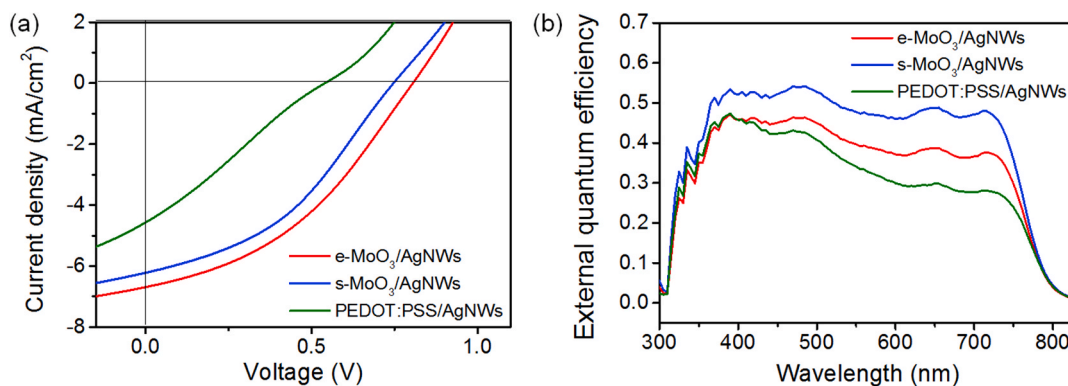


Fig. 4. *J-V* characteristics and EQE spectra of the full-coated devices with the structure of ITO/ZnO/PTB7-Th:PC₇₁BM/HTLs/Ag NWs.

Table 1

Device performance of the solar cells with different HTLs.

Structure	V _{oc} (V)	J _{sc} ^a (mA/cm ²)	FF	PCE (%)
e-MoO ₃ /e-Al	0.81	14.40	0.65	7.58
e-Al	0.42	10.40	0.2	0.87
e-MoO ₃ /p-AgNWs	0.80	10.08	0.39	3.14
s-MoO ₃ /p-AgNWs	0.78	12.20	0.44	4.19
PEDOT:PSS/p-Ag NWs	0.54	8.61	0.26	1.21

^a The J_{sc} values are calculated from EQE curves.

of 4.19% was obtained. In comparison with the e-MoO₃ HTL-based solar cell, we found a slightly lower V_{OC}, but a higher J_{SC} and FF for the s-MoO₃ HTL-based solar cells. The lower V_{OC} of s-MoO₃ cell might be due to relative lower work function of the solution-processed MoO₃ layer than the vacuum-evaporated MoO₃ [15,16]. On the side of higher J_{SC} and FF of the s-MoO₃ cell relative to the e-MoO₃ cell, it might be ascribed to the more robust properties to resist the solvent corrosion of such HTLs than the e-MoO₃ HTL. The photographs and atomic-force microscope (AFM) images of the active layer/HTL films before and after solvent treatment were measured to investigate the influence of solvent treatment. As shown by the photographs (Fig. S1) and AFM images (Fig. S2), we found the e-MoO₃ films were much smoother than the spray-coated MoO₃ films. After solvent wash, the e-MoO₃ film was partially destroyed and became rough. For the spray coated MoO₃ films, solvent wash caused much slight change though they were rougher. In addition, we use the PEDOT:PSS as the hole transport layer, realizing a PCE of 1.21%, a J_{sc} of 8.61 mA/cm², a V_{oc} of 0.54 V, and a FF of 0.26. The poor efficiency of the PEDOT:PSS-based solar cells also might be ascribed to the solvent effect since PEDOT:PSS is a core-shell structure aqueous with PEDOT and PSS as the core and shell, respectively. Because PEDOT and PSS are soluble in alcohol and water, respectively, so the spraying of IPA-dispersed Ag NWs on the top of PEDOT:PSS would partly dissolve

PEDOT, leading to the change of work function of the PEDOT:PSS HTL [17]. These results demonstrated the s-MoO₃ layer is more suitable to the full-coated OSCs. Herein, it is also worthy to note that the lower J_{SC} of the full-coated cell than the control cell was due to the high transparency of the top Ag NWs electrode. Thus, more light can't be harvest by these semi-transparent solar cells. The transmittance spectrum of the semitransparent solar cell with spray coated MoO₃ HTL and Ag NWs top electrode was showed in Figure S3. The average transmittance of the device from 300 to 800 nm was 24.8%.

3. Conclusion

To realize mass production of organic solar cells, blade-coating and spray-coating were integrated to realize vacuum-free fabrication. We demonstrate a fabrication method for all-solution vacuum-free organic solar cells on an assembled glass substrates. A gap-prefilling method was also developed to realize uniform thickness distribution. For the fully solution-processed devices, power conversion efficiency of 4.19% is obtained.

4. Experimental section

The device structure used in this work is ITO/ZnO/PTB7-Th (PBDTTT-EFT):PC₇₀BM/hole transport layer/anode. The prepatterned ITO glass substrates were cleaned with acetone, IPA and DI water for 15 min, respectively. The ITO substrates were treated by ultraviolet (UV) ozone for 15 min before ZnO deposition. The precursor of ZnO was prepared by dissolving zinc acetate dihydrate in 2-methoxyethanol (2-MOE) and ethanolamine (ETA). The blending ratio is zinc acetate:2-MOE:ETA = 40 mg:400 μl:11.2 μl. This precursor was blade coated on the substrate and baked at 100 °C for 1 h. The photoactive layer was prepared by blade coating a chlorobenzene solution of PTB7-Th

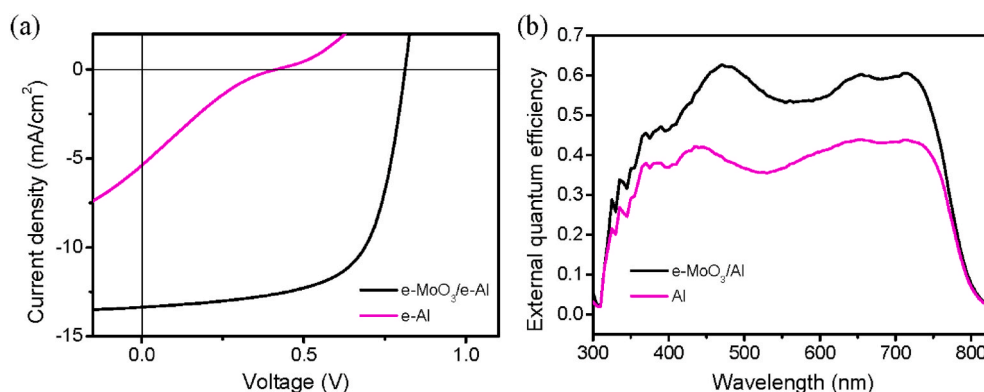


Fig. 5. *J-V* characteristics and EQE spectra of the reference devices. The anode for these devices are e-Al and e-MoO₃/e-Al.

(PBDTTT-EFT):PC₇₀BM on the substrate. The blending ratio is PTB7-Th (PBDTTT-EFT):PC₇₀BM:chlorobenzene = 10 mg:15 mg:1 ml. The active layer was put in vacuum for drying. Thermal-evaporated MoO₃ (e-MoO₃), spray-coated MoO₃ (s-MoO₃) and blade-coated PEDOT:PSS were used as hole transport layer for comparison. Ag nanowires (Ag NWS) was prepared by spray coating for comparing with thermal-evaporated Al. Film thickness was measured by ET-200 (Kosaka Laboratory Ltd.). The OPV devices were characterized by using a solar simulator (San-Ei Electric, XES 301S).

The s-MoO₃ nanoparticle ink was prepared through similar route reported by Xie et al. [13] with some modifications [14], and dispersed into ethanol with a concentration of 3 mg mL⁻¹. The Ag NWS (10 mg mL⁻¹ in isopropanol) were purchased from Blue nano with average diameter of 27 nm and 15 μm in length and diluted to 1.5 mg mL⁻¹ with ethanol before spray coating.

The s-MoO₃ HTL was spray coated on the active layer in the air with a spray coater (Hizenith AC300-1, Hizenith Robot (Suzhou) Co.,Ltd.) at a back pressure of 28 Pa. During the process of spray-coating, the nozzle moving speed was 14 mm s⁻¹, and the substrates were kept on a hotplate with 60 °C. The Ag NWS was spray coated on the s-MoO₃ HTL twice in the air with the same parameters.

The current density–voltage (*J*–*V*) curves were measured using a Keithley 2400 under simulated AM 1.5G sun light illumination (100 mW cm⁻²).

External quantum efficiencies (EQE) were measured under simulated one sun operation conditions using a bias light of 532 nm from a solid-state laser (Changchun New Industries, MGL–III–532). Light from a 150 W tungsten halogen lamp (Osram 64642) was used as probe light and modulated with a mechanical chopper before passing the monochromator (Zolix, Omni-I300) to select the wavelength. The response was recorded as the voltage by an *I*–*V* converter (QE-IV Converter, Suzhou D&R Instruments), using a lock-in amplifier (Stanford Research Systems SR 830). A calibrated Si cell was used as reference. The test device was kept behind a quartz window in a nitrogen filled container.

CRediT authorship contribution statement

Hao-Chun Yang: Methodology, Investigation. **Wusong Zha:** Methodology, Investigation. **Chia-Ning Weng:** Methodology, Investigation. **Chao-Hsuan Chen:** Methodology, Investigation. **Hsiao-Wen Zan:** Resources, Supervision. **Kuan-Wei Su:** Resources, Supervision. **Qun Luo:** Conceptualization, Writing - original draft, Writing - review & editing, Supervision. **Chang-Qi Ma:** Conceptualization, Resources, Writing - review & editing, Supervision. **Yu-Chiang Chao:** Conceptualization, Writing - original draft, Writing - review & editing, Supervision. **Hsin-Fei Meng:** Conceptualization, Resources, Writing - review & editing, Supervision.

Declaration of competing interest

The authors declare that they have no known competing financial interests or personal relationships that could have appeared to influence the work reported in this paper.

Acknowledgements

This work was supported by the Ministry of Science and Technology in Taiwan under contract number MOST 107-2119-M-009-005. This work was also supported by National Natural Science Foundation of China (51773224), Youth Innovation Promotion Association, CAS (2019317).

Appendix A. Supplementary data

Supplementary data to this article can be found online at <https://doi.org/10.1016/j.optmat.2020.110683>.

References

- [1] R. Xue, J. Zhang, Y. Li, Y. Li, *Small* 14 (2018) 1801793.
- [2] P.K. Nayak, S. Mahesh, H.J. Snaith, D. Cahen, *Nat. Rev. Mater.* 4 (2019) 269–285.
- [3] D.D.C. Rasi, R.A.J. Janssen, *Adv. Mater.* 31 (2019) 1806499.
- [4] J.J. van Franeker, W.P. Voorthuijzen, H. Gorter, K.H. Hendriks, R.A.J. Janssen, A. Hadipour, R. Andriessen, Y. Galagan, *Sol. Energy Mater. Sol. Cells* 117 (2013) 267–272.
- [5] S. Berny, N. Blouin, A. Distler, H. Egelhaaf, M. Krompiec, A. Lohr, O.R. Lozman, G. E. Morse, L. Nanson, A. Pron, T. Saueremann, N. Seidler, S. Tierney, P. Tiwana, M. Wagner, H. Wilson, *Adv. Sci.* 3 (2016) 1500342.
- [6] K.M. Huang, Y.Q. Wong, M.C. Lin, C.H. Chen, C.H. Liao, J.Y. Chen, Y.H. Huang, Y. F. Chang, P.T. Tsai, S.H. Chen, C.T. Liao, Y.C. Lee, L. Hong, C.Y. Chang, H.F. Meng, Z. Ge, H.W. Zan, S.F. Horng, Y.C. Chao, H.Y. Wong, *Prog. Photovoltaics Res. Appl.* 27 (2018) 264–274.
- [7] Y. Zhao, G. Wang, Y. Wang, T. Xiao, M.A. Adil, G. Lu, J. Zhang, Z. Wei, *Sol. RRL* 3 (2019) 1800333.
- [8] S. Hong, H. Kang, G. Kim, S. Lee, S. Kim, J.H. Lee, J. Lee, M. Yi, J. Kim, H. Back, J. R. Kim, K. Lee, *Nat. Commun.* 7 (2016) 10279.
- [9] C. Giroto, D. Moia, B.P. Rand, P. Heremans, *Adv. Funct. Mater.* 21 (2011) 64–72.
- [10] K.M. Huang, C.M. Lin, S.H. Chen, C.S. Li, C.H. Hu, Y. Zhang, H.F. Meng, C. Y. Chang, Y.C. Chao, H.W. Zan, L. Huo, P. Yu, *Sol. RRL* 3 (2019) 1900071.
- [11] G. Ji, Y. Wang, Q. Luo, K. Han, M. Xie, L. Zhang, N. Wu, J. Lin, S. Xiao, Y.Q. Li, L. Q. Luo, C.Q. Ma, *ACS Appl. Mater. Interfaces* 10 (2018) 943–954.
- [12] T. Lei, R. Peng, W. Song, L. Hong, J. Huang, N. Feia, Z. Ge, *J. Mater. Chem.* 7 (2019) 3737–3744.
- [13] F. Xie, W.C.H. Choy, C. Wang, X. Li, S. Zhang, J. Hou, *Adv. Mater.* 25 (2013) 2051–2055.
- [14] Y. Wang, Q. Luo, N. Wu, Q. Wang, H. Zhu, L. Chen, Y.Q. Li, L. Luo, C.Q. Ma, *ACS Appl. Mater. Interfaces* 7 (2015) 7170–7179.
- [15] X. Zhang, F. You, Q. Zheng, Z. Zhang, P. Cai, X. Xue, J. Xiong, J. Zhang, *Org. Electron.* 39 (2016) 43–49.
- [16] I. Ahmad, A. Turinske, Z. Bao, Y. Gao, *Appl. Phys. Lett.* 101 (2012), 093305.
- [17] M.H. Lee, L. Chen, N. Li, F. Zhu, *J. Mater. Chem. C* 5 (2017) 10555–10561.